NeuroImage 84 (2014) 488–494

Contents lists available at ScienceDirect

NeuroImage

journal homepage: www.elsevier.com/locate/ynimg

Subsequent memory effect in intracranial and scalp EEG

Nicole M. Long [a], John F. Burke [b], Michael J. Kahana [a,b,*]

[a] Department of Psychology, University of Pennsylvania, Philadelphia, PA 19104, USA
[b] Neuroscience Graduate Group, University of Pennsylvania, Philadelphia, PA 19104, USA

ARTICLE INFO

Article history:
Accepted 26 August 2013
Available online 6 September 2013

Keywords:
EEG
iEEG
Free-recall
Memory

ABSTRACT

Successful memory encoding is marked by increases in 30–100 Hz gamma-band activity in a broad network of brain regions. Activity in the 3–8 Hz theta band has also been shown to modulate memory encoding, but this effect has been found to vary in direction across studies. Because of the diversity in memory tasks, and in recording and data-analytic methods, our knowledge of the theta frequency modulations remains limited. The difference in the directionality of these theta effects could arise from a distinction between global cortical and deeper subcortical effects. To address this issue, we examined the spectral correlates of successful memory encoding using intracranial EEG recordings in neurosurgical patients and scalp EEG recordings in healthy controls. We found significant theta (3–8 Hz) power modulations (both increases and decreases) and high gamma (44–100 Hz) power increases in both samples of participants. These results suggest that (1) there are two separate theta mechanisms supporting memory success, a broad theta decrease present across both the cortex and hippocampus as well as a theta power increase in the frontal cortex, (2) scalp EEG is capable of resolving high frequency gamma activity, and (3) iEEG theta effects are likely not the result of epileptic pathology.

© 2013 Elsevier Inc. All rights reserved.

Introduction

Memory processes during encoding that give rise to successful retrieval are collectively termed subsequent memory effects (SMEs, Paller and Wagner, 2002) and have been characterized using scalp electroencephalography (EEG, Paller et al., 1987; Klimesch et al., 1997; Sederberg et al., 2006), magnetoencephalography (MEG, Osipova et al., 2006; Guderian et al., 2009), and intracranial EEG recorded in neurosurgical patients undergoing treatment for intractable epilepsy (iEEG, Fernandez et al., 1999; Fell et al., 2001; Sederberg et al., 2003). Whereas these recording modalities have millisecond temporal resolution, scalp EEG is limited by poor spatial resolution and may not reveal changes in high frequency activity due to muscle and eye movement artifacts that generate their own high frequency electrical signals (Yuval-Greenberg et al., 2008; Muthukumaraswamy, 2013). In comparison, iEEG offers subcentimeter range spatial resolution and the ability to directly record from deep brain structures. However, iEEG can only be recorded in neurosurgical patients leading some to question the generalizability of these results to neurologically healthy individuals.

Both iEEG and scalp EEG have been effectively used to study the spectral correlates of memory encoding. Although most studies show gamma (30–100 Hz) power increases for subsequent memory (Gruber et al., 2004; Sederberg et al., 2006; Osipova et al., 2006; Serruya et al., in press), direct comparisons cannot be easily made because of differences in experimental and data analytic methods. For example, Morton et al. (in press) measured category-specific oscillatory patterns and found that high gamma was more informative in iEEG than scalp EEG. However, the scalp study included a preliminary session in which participants rated the familiarity of the experimental stimuli. As gamma effects are often observed for primacy items (Sederberg et al., 2006; Serruya et al., in press), pre-exposure to the items may have dampened potential scalp gamma effects.

Theta frequency (3–8 Hz) activity has exhibited both increases and decreases during successful memory formation (Burgess and Gruzelier, 1997; Klimesch, 1999; Sederberg et al., 2003, 2006; Osipova et al., 2006; Guderian et al., 2009; Lega et al., 2011; Hanslmayr and Staudigl, in press). The inconsistent patterns observed in the theta band could arise from a number of factors including the task parameters and the brain regions, time windows, and frequencies analyzed. For example, there may be differential effects of theta power based on anatomical location, with the hippocampus showing an increase in theta power and neocortical regions showing decreases (Lisman and Jensen, 2013).

Our goal here is to compare the spectral SMEs measured using both intracranial and scalp EEG by controlling as many of these variables as possible. Using identical data analytic methods and roughly corresponding brain regions, we analyzed data from neurosurgical patients (n = 93) and healthy participants (n = 102) who participated in a free recall study. To foreshadow our results, we found very similar patterns of results in both iEEG and scalp EEG indicating that memory

* Corresponding author at: Department of Psychology, University of Pennsylvania, 3401 Walnut Street, Room 316C, Philadelphia, PA 19104, USA. Fax: +1 215 746 3848.
E-mail address: kahana@psych.upenn.edu (M.J. Kahana).

1053-8119/$ – see front matter © 2013 Elsevier Inc. All rights reserved.
http://dx.doi.org/10.1016/j.neuroimage.2013.08.052

effects observed in iEEG can be directly translated to healthy individuals and that high frequency effects can be detected by scalp EEG.

iEEG methods

Participants

98 participants with medication-resistant epilepsy underwent a surgical procedure in which electrodes were implanted subdurally on the cortical surface as well as deep within the brain parenchyma. In each case, the clinical team determined the placement of the electrodes so as to best localize epileptogenic regions. Demographic and electrode information are described in publications on the same dataset (Burke et al., in press).

Data were collected at 4 hospitals: Boston Children's Hospital (Boston, MA), Hospital of the University of Pennsylvania (Philadelphia, PA), Freiburg University Hospital (Freiburg, Germany), and Thomas Jefferson University Hospital (Philadelphia, PA). The research protocol was approved by the IRB at each hospital and informed consent was obtained from the participants and their guardians. We restricted our analysis to include only those patients ($n = 93$) who were left-hemispheric language dominant, as assessed by either the patients' handedness or a clinically administered intracarotid injection of sodium amobarbital (Wada test). As the electrode placements in these 93 patients were clinically determined, each patient did not have electrodes in all of our regions of interest (see below). Therefore, the total number of patients per region of interest varied as a function of electrode placement; the total number of patients for a given region of interest ranged from 29 (left inferior prefrontal cortex) to 55 (non-hippocampal medial temporal lobe cortex).

Experimental paradigm

Each patient participated in a delayed free-recall task in which they were instructed to study lists of words for a later memory test; no encoding task was used. Lists were composed of either 15 (67/93 patients) or 20 common nouns, chosen at random and without replacement from a pool of high frequency nouns (either English or German, depending on the patient's native language; http://memory.psych.upenn.edu/WordPools). Each sequentially presented word remained on the screen for 1600 ms, followed by a randomly jittered 800–1200 ms blank inter-stimulus interval (ISI).

Immediately following the final word in each list, participants were given a distraction task designed to attenuate the recency effect (Kahana, 2012). The distraction task was a series of arithmetic problems of the form $A + B + C = ??$, where A, B and C were randomly chosen integers ranging from 1 to 9. The distraction interval lasted at least 20 s, but patients were allowed to complete any problem that they started resulting in a variable distraction interval (average duration, 25 s).

Following the distraction period, participants were given 45 s to freely recall as many words as possible from the list in any order. Vocalizations were digitally recorded and subsequently manually scored for analysis. On average, patients participated in two sessions yielding an average total of 14 lists. Any session in which probability of recall was less than 15% was excluded from the final analysis, resulting in an average of one session per patient.

Electrophysiological recordings and data processing

iEEG data were recorded using a Bio-Logic, DeltaMed, Nicolet, GrassTelefactor, or Nihon Kohden electroencephalogram (EEG) system. Depending on the amplifier and the discretion of the clinical team, the signals were sampled at 256, 400, 500, 512, 1000, 1024, or 2000 Hz. Signals were referenced to a common contact placed either intracranially or on the scalp or mastoid process.

Scalp methods

Participants

102 (60 female) paid volunteers (ages 18–29), were recruited via fliers posted around the University of Pennsylvania campus. Participants were provided with a base monetary compensation plus an additional performance-based monetary incentive to ensure full effort. Our research protocol was approved by the Institutional Review Board at the University of Pennsylvania, and informed consent was obtained from all participants.

Experimental paradigm

The data reported in this manuscript were collected as part of the Penn Electrophysiology of Encoding and Retrieval Study, involving three experiments that were sequentially administered. The data reported here come from participants who took part in Experiment 1. The methods are briefly summarized below, and a complete description of the methods can be found in Lohnas and Kahana (in press) and J. F. Miller et al. (2012).

Each session consisted of 16 lists of 16 words presented one at a time on a computer screen. Each study list was followed by an immediate free recall test.

The study also included an encoding task manipulation: some lists were encoded freely (no-task lists) whereas other lists were encoded using a size or animacy task (i.e. will the item fit in a shoebox? Is it living or non-living?). To facilitate comparison between scalp EEG and iEEG studies, we only considered the "no-task" lists in these analyses.

Words were drawn from a pool of 1638 words (http://memory.psych.upenn.edu/Word_Pools). Each item was on the screen for 3000 ms, followed by a randomly jittered 800–1200 ms inter-stimulus interval. After the last item in the list, there was a 1200–1400 ms jittered delay, after which a tone sounded, a row of asterisks appeared, and the participant was given 75 s to attempt to recall any of the just-presented items.

To maintain consistency with the iEEG dataset, we only analyzed the first 1600 ms of word presentation. As the scalp paradigm utilized immediate free recall, to further constrain the comparison, we excluded words from late serial positions (13–16) to minimize effects of recency. Additionally, each participant completed seven experimental sessions; however, to more closely match the iEEG dataset and reduce the influence of practice effects, we only analyzed the first 4 sessions. It was with this number of sessions that iEEG and scalp EEG datasets had on average an equal number of recall events.

Electrophysiological recordings and data processing

EEG measurements were recorded using Geodesic Sensor Nets (GSN; Netstation 4.3 acquisition environment, from Electrical Geodesics, Inc.). The GSN provided 129 standardized electrode placements across participants. All channels were digitized at a sampling rate of 500 Hz, and the signal from the caps was amplified via either the Net Amps 200 or 300 amplifier. Recordings were initially referenced to Cz and later converted to an average reference. Channels that demonstrated high impedance or poor contact with the scalp were excluded from the average reference.

To identify epochs contaminated with eyeblink and other movement artifacts, electrooculogram (EOG) activity was monitored bipolarly using right and left electrode pairs (electrodes 25, 127 and 8 and 126 on the GSN). An individual word presentation event was rejected from subsequent analyses if the weighted running average for either the right or the left EOG pair exceeded a 100 μV threshold. Additionally, events were excluded on a per channel basis for each participant if the voltage on a particular event/channel pair exceeded a predetermined threshold. The threshold was set as 4.5 times the standard deviation of the mean voltage calculated across all electrodes (excluding

those on the eyes, face and neck, electrodes F10, 8, FPZ, 17, FPZ, 25, F9, T9, 56, 63, 99, 107, 113, T10, 126, 127) for a single session for each participant.

Analysis of iEEG and scalp EEG data

Behavioral analysis

We calculated probability of recall as well as the number of intrusions, or incorrect recalls, for participants in both datasets. Intrusions were measured for each participant and each list by calculating the number of incorrect words recalled (words not from the preceding study list) as a proportion of the total number of words recalled. Values were then averaged across lists for each participant.

Oscillatory analysis

To minimize confounds resulting from volume conduction and saccades, we analyzed both the iEEG and scalp EEG with bipolar referencing (Nunez and Srinivasan, 2006; Kovach et al., 2011). We defined the bipolar montage in our dataset based on the geometry of the iEEG and scalp EEG electrode arrangements. For each participant and electrode, the raw EEG signal was first downsampled to 200 Hz and a fourth order 2 Hz stopband butterworth notch filter was applied at 50 or 60 Hz to eliminate electrical line noise. We isolated pairs of immediately adjacent electrodes and found the difference in voltage between them (Burke et al., 2013, in press). The resulting bipolar signals were treated as new virtual electrodes and are referred to as such in the remainder of the text. The Morlet wavelet transform (with a wave number of 6) was used to compute spectral power as a function of time for all EEG signals during word presentation (0–1600 ms) and a 1000 ms buffer was included on both sides of the data to minimize edge effects. Frequencies were sampled logarithmically at 46 intervals between 2 and 100 Hz. Power values were then down-sampled by taking a moving average across 100 ms time windows from stimulus onset and sliding the window every 50 ms, resulting in 31 total time windows with 16 non-overlapping time windows.

Log transformed power values were then Z-transformed to normalize power within participants. Power was Z-transformed according to the mean and standard deviation of the power across all events within a session, separately for each participant, electrode and frequency.

ROI selection and analysis

iEEG ROIs were selected a priori by Brodmann area or gyrus. We were interested in regions most commonly associated with memory encoding and retrieval (Wagner et al., 1998; Blumenfeld and Ranganath, 2007; Sederberg et al., 2007; Shrager et al., 2008; Kim, 2011), and therefore chose the following eight ROIs: bilateral inferior temporal cortex (BA 20, 21), bilateral inferior frontal cortex (IFC, BA 45, 47), bilateral dorsolateral prefrontal cortex (DLPFC, BA 46, 9), bilateral hippocampus and parahippocampal cortex. Localizations were radiologically determined by a neurologist at each of the four hospitals. The number of participants with at least one electrode in each of these regions is in parentheses in Table 1A. Scalp ROIs were selected a priori (Weidemann et al., 2009) to loosely match the cortical iEEG ROIs with bilateral anterior superior (AS, corresponding to DLPFC), bilateral anterior inferior (AI, corresponding to IFC), and bilateral posterior inferior (PI, corresponding to inferior temporal). Fig. 1 shows both iEEG and scalp EEG topographies for the current study.

Frequency effects across time

The data were split into five distinct bands, theta (3 to 8 Hz), alpha (10 to 14 Hz), beta (16 to 26 Hz), low gamma (28 to 42 Hz) and high gamma (44 to 100 Hz), by taking the mean of the Z-transformed power in each frequency band. Z-transformed power was filtered into the conditions being analyzed (e.g. subsequently recalled and subsequently forgotten events) and an unpaired *t*-test was run comparing the two sets of events separately for each participant, electrode and frequency band across the 1600 ms duration of encoding word presentation. *t*-Statistics were then averaged across electrodes within an ROI. Averaging *t*-statistics means that only signals that are consistent across an ROI will appear significant, as opposing effects will be canceled out. We chose this method as we were interested in general effects across an ROI and not regional differences within an ROI. This averaging step yielded a single *t*-statistic for each participant and frequency band for a given ROI. Within an ROI and for a particular frequency band, an unpaired *t*-test was calculated across the participant *t*-statistics. All resultant *t*-statistics are presented in Table 1.

Table 1
T-statistics for the comparison of z-scored power for recalled–not recalled items, across the five frequency bands and for (A) iEEG cortical, (B) Scalp, and (C) iEEG subcortical ROIs. Numbers in parentheses denote number of participants with electrodes in each region. $^{*}p < .05$, $^{**}p < .01$.

	A. iEEG		B. Scalp	
	DLPFC		AS	
	Left (31)	Right (42)	Left (102)	Right (102)
Theta	−2.44*	−5.56**	−1.30	−2.65**
Alpha	−3.99**	−1.93	−3.69**	−4.54**
Beta	−4.01**	−1.95	−2.41*	−1.81
Gamma1	2.23*	−0.43	0.01	−0.31
Gamma2	3.58**	1.44	1.35	1.35
	IFC		AI	
	Left (29)	Right (38)	Left (102)	Right (102)
Theta	−2.39*	−4.02**	−0.85	−1.58
Alpha	−2.66*	−2.53*	−3.65**	−2.97**
Beta	−3.19**	−1.80	−2.37*	−1.86
Gamma1	−0.38	−0.35	−0.93	−0.96
Gamma2	1.70	1.49	0.20	−0.09
	InfTem		PI	
	Left (52)	Right (51)	Left (102)	Right (102)
Theta	−6.16**	−3.49**	−3.20**	−2.29*
Alpha	−6.74**	−3.76**	−4.08**	−3.69**
Beta	−4.56**	−3.78**	−0.37	−0.35
Gamma1	1.24	−1.48	0.84	1.08
Gamma2	4.54**	1.99	1.48	1.48
	C. iEEG subcortical			
	Hippocampus (47)		MTL (55)	
Theta	−3.60**		−5.92**	
Alpha	−4.12**		−5.76**	
Beta	−2.63*		−1.98	
Gamma1	−.14		2.86**	
Gamma2	2.23*		4.18**	

In cases in which we ran post-hoc tests on z-scored power to determine the laterality of frequency effects, we used a Bonferroni corrected *p* value.

Time-frequency analysis

We used a modified version of the bootstrap method detailed in previous studies (Sederberg et al., 2006; Serruya et al., in press). We corrected for comparisons across 16 time windows and 46 frequencies.

For each participant, electrode, time window and frequency, a *t*-statistic was generated through an unpaired *t*-test comparing the z-scored power of subsequently recalled to not recalled items. These *t*-statistics were averaged across electrodes within an ROI, creating a single *t*-statistic for each participant, time window and frequency for one ROI. The distribution of participant *t*-statistics was compared to zero using an unpaired *t*-test, resulting in a single across participant *t*-statistic for each time window and frequency. To correct for multiple comparisons, we ran a bootstrap procedure in which we generated a null distribution of across participant *t*-statistics. For the bootstrap analysis, we followed the same procedure as above, however, the tests were

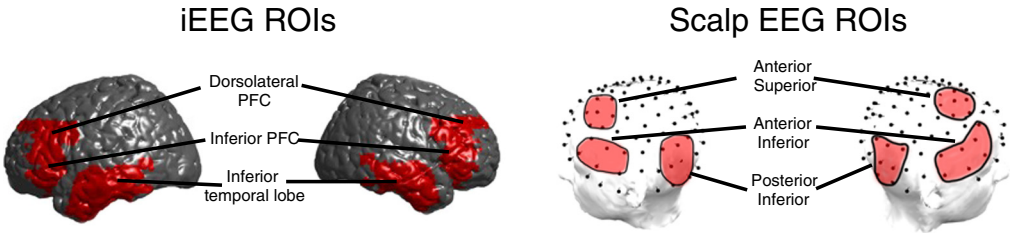

Fig. 1. Maps of a priori selected regions of interest.

carried out on shuffled data, such that the labels of subsequently recalled and not recalled were randomly assigned to events. Instead of a single across participant *t*-statistic being generated, 1000 null across participant *t*-statistics were generated from 1000 iterations of the bootstrap procedure. Finally, all null *t*-statistics from the 16 time windows and 46 frequencies were concatenated into a single distribution of 736,000 values. To determine which real *t*-statistics, and thus time windows and frequencies, were significant at a $p = .05$ level corrected for multiple comparisons, we found the top and bottom 2.5% of the null distribution. Any real *t*-statistics which exceeded those values were labeled significant and the corresponding z-scored power differences (subsequently recalled–not recalled) appear in the time frequency plots in Fig. 3.

In cases in which we ran post-hoc tests on z-scored power to determine the temporal or regional specificity of frequency effects, we used a Bonferroni corrected *p* value.

Results

Before examining the spectral components of the subsequent memory effect, we report the basic behavioral data for the two studies. In the scalp EEG study, participants recalled an average of 68% of the studied items (SD = 14%) and committed an average of .31 recall errors (0.12 prior list intrusions [$SD = .09$] and 0.19 extra list intrusions [$SD = .17$]) on each list. Neurosurgical patients who participated in the iEEG study recalled an average of 24% of studied items (SD = 9%) and committed an average of 4.2 recall errors (0.64 prior list intrusions [$SD = .63$] and 3.57 extra list intrusions [$SD = 3.58$]) per list. The finding of substantially lower recall and higher intrusion rates in the iEEG study was to be expected both because the task was inherently more difficult (delayed free recall for the iEEG participants vs. immediate free recall for the scalp EEG participants) and because of the obvious differences in the populations being studied (a community sample of neurosurgical patients with medial temporal lobe epilepsy vs. an elite college population). We also obtained a measure of general intelligence (Wechsler Adult Intelligence Scale) for 77 of the scalp EEG participants and 74 of the iEEG participants. As expected IQ scores for the scalp EEG participants ($M = 128$, $SD = 10$) were substantially higher than for the iEEG participants ($M = 98$, $SD = 14$).

We characterized the spectral components of the SME by comparing power in five frequency bands (theta, alpha, beta, low and high gamma) across items subsequently recalled and subsequently forgotten across the presentation interval (1600 ms). The comparison of subsequently recalled minus not recalled items revealed low frequency power decreases and high frequency power increases (Figs. 2A–C). We found significant theta and alpha power decreases across all ROIs with the exception of a nonsignificant alpha effect in right DLPFC (Table 1A–C). Beta power was significantly decreased across most ROIs except right DLPFC, bilateral PI, right AS, right AI, and parahippocampus.

Gamma effects were less widespread with significant high gamma increases predominantly localized to the left hemisphere, including left DLPFC and left inferior temporal cortex (Fig. 2A). Gamma effects were also evident in both hippocampal and parahippocampal ROIs (Fig. 2). To test the apparent gamma laterality in iEEG we ran paired *t*-tests comparing high gamma power across the three pairs of left and right ROIs in those participants with at least one electrode in each ROI. Gamma power in left DLPFC was significantly more increased than in the right ($t(17) = 3.4$, $p = .004$; critical *p*-value set at 0.02; Bonferroni corrected 0.05/3).

Temporal dynamics of the subsequent memory effect

One of the main benefits of EEG data is its high temporal resolution. Subtle effects that may exist on smaller time scales could be obscured by collapsing data across large time intervals (as above). Though not observed when time intervals were collapsed, when examining 100 ms windows between 0 and 1600 ms, we found significant theta power increases in left DLPFC, bilateral AI, and right PI around 500 ms (Figs. 3A–B). This theta power increase was not specifically left- or right-lateralized for either iEEG or scalp ROIs, as revealed by paired *t*-tests comparing theta power differences from 400 to 600 ms in left and right DLPFC and PI in those participants with at least one electrode in each ROI ($ts < 2$, $ps > .1$ critical *p*-value set at 0.03; Bonferroni corrected 0.05/2).

All ROIs, including hippocampus, showed late theta decreases (Figs. 3A–C). We ran a 6 × 2 repeated measures ANOVA on the scalp EEG z-scored theta power comparing all 6 ROIs and 2 time windows (early, 0–500 and late, 1000–1500 ms). This analysis revealed no main effect of ROI ($F(5,505) = 1.6$, $p = .2$), a main effect of time window ($F(1,101) = 19.5$, $p < .0001$), and no interaction ($F(5,1111) = 2.2$, $p = .06$). A post-hoc *t*-test of z-scored theta power averaged across all ROIs revealed that theta power was significantly decreased in the late time window relative to the early time window ($t(101) = 4.4$, $p < .0001$). To assess the temporal dynamics of z-scored theta power in the iEEG dataset we ran paired *t*-tests comparing theta power from 0–500 ms and 1000–1500 ms in each ROI, as not all participants contributed electrodes to all ROIs. Theta was significantly decreased in the late time window for all ROIs ($ts > 3.0$, $ps < .005$, critical *p*-value set at .006, Bonferroni corrected .05/8) except left DLPFC ($t(30) = 2.4$, $p = .02$).

Increased temporal precision showed that gamma power increases were present both in iEEG and scalp EEG (Figs. 3A–C). We ran a 6 × 2 repeated measures ANOVA on the scalp EEG z-scored gamma power comparing all 6 ROIs and 2 time windows (early, 0–500 and late, 1000–1500 ms). This analysis revealed no main effect of ROI ($F(5,505) = .91$, $p = .48$), a main effect of time window ($F(1,101) = 19.0$, $p < .0001$), and no interaction ($F(5,1111) = 1.9$, $p = .1$). A post-hoc *t*-test of z-scored gamma power averaged across all ROIs revealed that gamma power was significantly increased in the early time window relative to the late time window ($t(101) = 4.4$, $p < .0001$). To assess the temporal dynamics of z-scored gamma power in the iEEG dataset we ran paired *t*-tests comparing gamma power from 0–500 ms and 1000–1500 ms in each ROI, as not all participants contributed electrodes to all ROIs. Gamma was significantly increased in the late time window for left DLPFC and left IFC ($ts > 3.5$, $ps < .006$, critical *p*-value set at .006, Bonferroni corrected .05/8). There was no significant

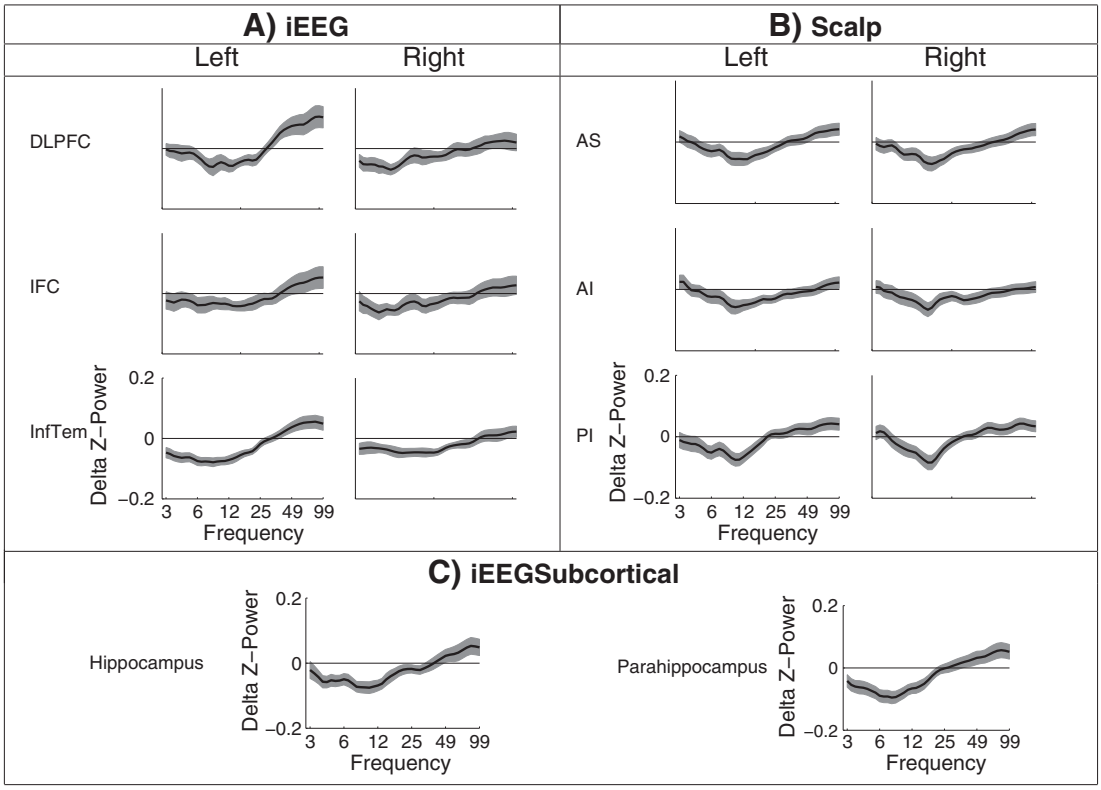

Fig. 2. Z-scored power for recalled minus not recalled items for all frequencies (3 to 100 Hz) and collapsed across 1600 ms for (A) iEEG Cortical, (B) scalp, and (C) iEEG Subcortical ROIs. Shaded regions around each curve are Loftus Masson 95% confidence intervals.

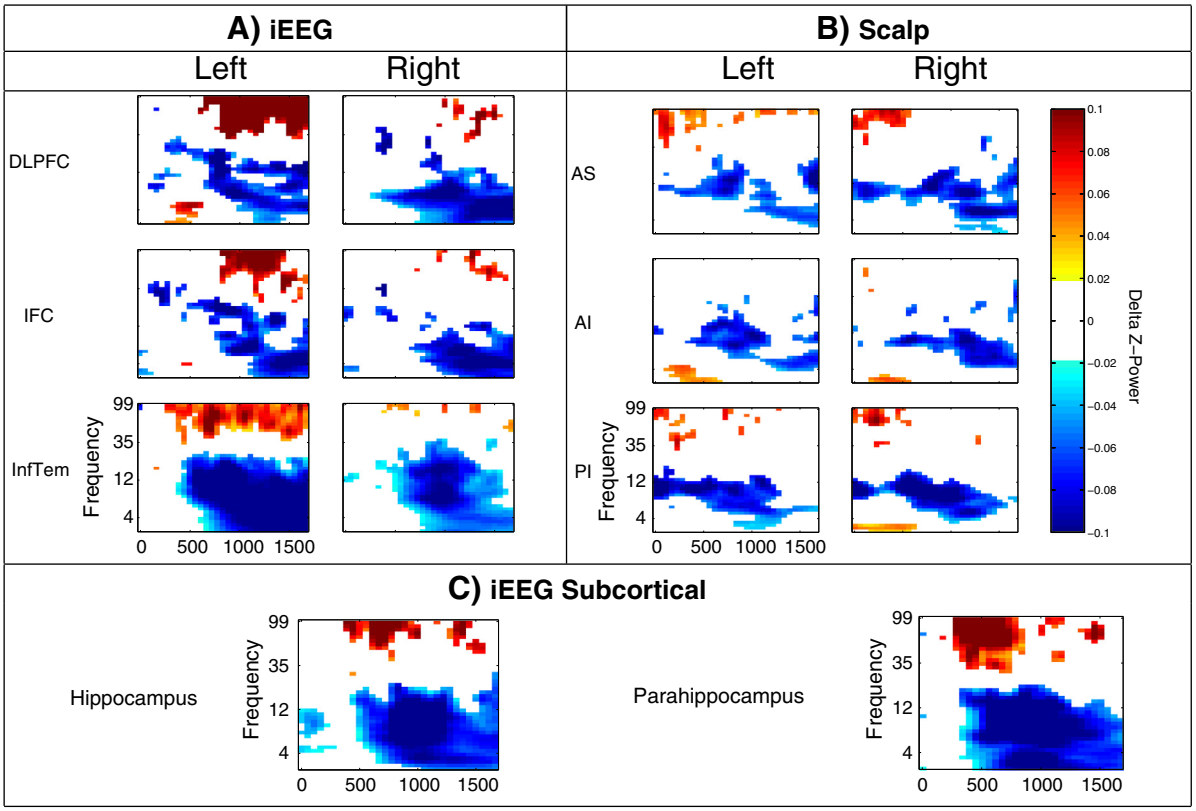

Fig. 3. Time frequency spectrograms for recalled minus not recalled z-scored power for all frequencies (3 to 100 Hz) and across 100 ms time windows spanning 0 to 1600 ms for (A) iEEG cortical, (B) scalp, and (C) iEEG subcortical ROIs. All time-frequency pairs of z-power values were tested using a bootstrap procedure (see Analysis of iEEG and scalp EEG data) and any area in white did not pass the significance threshold of $p = .05$ corrected for multiple comparisons.

difference in gamma power for the remaining ROIs (right DLPFC, right IFC, bilateral IT, hippocampus or PHC, $ts < 2.5$, $ps > .03$).

Discussion

Memory formation elicited a remarkably similar pattern of results across scalp and iEEG recordings. Across the encoding interval a general pattern of low frequency decreases and high frequency increases was present in both datasets. While theta power decreases and gamma power increases were evident across the encoding interval, a more precise examination of the temporal dynamics revealed theta increases in addition to the decreases. iEEG and scalp EEG showed significant theta increases around 500 ms post stimulus onset. That both effects predominantly localized to the frontal region suggests that they may reflect the 'frontal mid-line (FM) theta' pattern often observed during cognitive tasks (for a comprehensive review, see Mitchell et al., 2008). The origin of FM theta in human EEG recording is unclear; midline frontal areas, such as the anterior cingulate cortex (ACC), are most commonly cited as potential sources (Gevins et al., 1997; Sauseng et al., 2007) and might explain the lack of a laterality effect in the current study. Additionally, there is evidence that though generated in medial PFC, frontal midline theta extends outward into a network of regions encompassing lateral PFC (Mizuhara et al., 2004). Our results show that these theta increases are conserved across both iEEG and scalp EEG and are consistent with other scalp EEG studies showing theta power increases (Klimesch et al., 1997, 1998; Hanslmayr et al., 2011).

In addition to very circumscribed theta power increases in frontal cortex, we also observed broad theta power decreases across iEEG and scalp EEG, including hippocampus. There are two hypotheses to explain the decreases in theta power. First, it has been suggested (Stoller, 1949) that theta decreases in iEEG reflect decreases in alpha power as the alpha rhythm may be slowed in epileptic brains. However, we found highly similar theta power decreases in healthy controls in the scalp study, suggesting that theta power decreases in iEEG are not an artifact of the patient population. A second hypothesis is that theta power decreases and increases are separate properties of the neocortex and the hippocampus, respectively (Lisman and Jensen, 2013). However, we observe the same decreases across both neocortical and hippocampal ROIs, which runs counter to this hypothesis. Previous work using a subset of the data presented here (Lega et al., 2011) has shown theta power increases in the hippocampus for subsequently remembered items. While the current study does not show this effect, it is likely due to the fact that Lega et al. (2011) specifically regressed out broadband shifts in spectral power in order to detect oscillations. As broadband activity is known to correlate with local field potentials (Manning et al., 2009) and could potentially be related to memory signals, we did not wish to bias ourselves to only detecting oscillations. Additionally, while Lega et al. (2011) specifically focused on theta power increases, they also observed significant theta power decreases that occurred roughly twice as often as theta power increases (cf Figs. 2A and 3 in Lega et al.), consistent with the results reported here.

We hypothesize that these conflicting results of theta power increases and decreases reflect two competing effects: shifts in broadband power and narrow-band theta oscillations, leading to subsequent memory effects characterized either by theta power decreases or increases, respectively. Furthermore, broadband power shifts appear to be much larger than narrow-band changes, resulting in the overall decrease in theta power reported here and in other studies (Sederberg et al., 2007; Guderian et al., 2009; Burke et al., 2013, in press). However, when these broadband power changes are removed, as in Lega et al. (2011), increases in theta power are more readily observed. Consistent with the hypothesis of two separate theta effects, Burke et al. (2013, in press) recently found that theta synchrony, presumably a more specific marker of theta oscillatory activity, exhibits both increases and decreases during memory formation.

One limitation of the current study is the use of a single task, free recall, to measure encoding processes. It is possible that the effects observed may be specific to free recall and thus may not be observed across other memory paradigms or with an analysis comparing different sets of events as opposed to subsequently recalled and not recall items (Hanslmayr and Staudigl, in press). However, there is some evidence that theta power decreases and gamma power increases are task independent memory signals as this pattern has been observed in a subsequent memory study utilizing recognition (Matsumoto et al., 2013). Our results provide compelling evidence to motivate future memory studies to investigate the role of theta power in memory processes.

Although we have presented topographies of the subsequent memory effect across scalp and intracranial datasets for roughly corresponding regions of interest, we fully recognize that scalp EEG does not permit the identification of signal generating sources with anywhere near the precision of subdural electrode recordings. Indeed, given the difference in timing of memory-related gamma-band activity (discussed below), frontal gamma effects in scalp are potentially more related to activity in the medial temporal lobe.

In addition to late low frequency decreases, both iEEG and scalp EEG showed high frequency increases. In iEEG, significant gamma power increases were evident across the encoding interval for left cortical and all subcortical ROIs. The time frequency analysis revealed that these effects were present across the 1600 ms encoding interval for all ROIs with the exception of left DLPFC and left IFC which showed significantly greater gamma power in the late (1000–1500 ms) time window. In comparison, significant gamma effects were not present across the encoding interval for the scalp EEG dataset, although gamma effects were typically in the positive direction. The time frequency analysis revealed significant gamma effects across all ROIs for the early (0–500 ms) time window.

As gamma is considered a mapping signal related to the BOLD activation observed with fMRI (Crone et al., 2011; Lachaux et al., 2012; Burke et al., in press), we would expect that the gamma effects in iEEG would closely mirror the subsequent memory effects observed with fMRI. Scalp EEG, due to its low spatial resolution, would be less likely to map directly onto the signals observed in fMRI and iEEG. The significant gamma results in scalp EEG suggest that despite concerns about interference from eye and muscle movement (Yuval-Greenberg et al., 2008; Muthukumaraswamy, 2013), which may still be present here, as well as general attenuation of spectral power due to the skull (Voytek et al., 2010), scalp EEG is able to resolve high frequency gamma effects, at least up to 100 Hz.

It is clear from our results that across both intracranial and scalp EEG the dominant electrophysiological effect of successful memory encoding is an overall skew in power toward higher-frequencies at the expense of lower-frequencies. The meaning of this pattern vis-a-vis episodic memory is an open question, but we note that a similar pattern of results is found across a wide variety of electrophysiological recordings during behaviors ranging from motor movement (K. J. Miller et al., 2007; Crone et al., 1998a, 1998b) to auditory tone perception (Crone et al., 2001), among others. Indeed, this pattern is consistent with the event-related synchronization/desynchronization (ERS/ERD) processes that have been described outside of the memory literature (see Pfurtscheller and Lopes Da Silva, 1999 for a review). Furthermore, recent studies have found that this pattern of spectral changes correlates well with the fMRI BOLD signal (Kilner et al., 2005; Niessing et al., 2005). Our results show that this pattern is fairly conserved across the brain, for both iEEG and scalp EEG, given that low frequency power decreases and high frequency power increases are observed with slight variation across all ROIs. It is therefore possible that the spectral content of both iEEG and scalp EEG during memory formation may not reflect a memory specific signal per se, but rather may indicate a more non-specific underlying process of general cortical activation and that it is the precise intersection of timing and spatial location of these effects that is important.

Beyond this characterization of memory processes, these results suggest that while data from individual patients might not be reflective of normal functioning, the average effects across a large patient population are representative of the general population. Additionally, these results suggest that, despite its limited spatial resolution and potential muscle artifacts, scalp EEG measures qualitatively similar physiological processes as more precise yet more invasive recording techniques.

Funding

This work was supported by the National Institutes of Health (grant numbers MH061975, MH055687).

Acknowledgments

We thank Kylie Hower, Joel Kuhn, Elizabeth Crutchley, and Ryan Williams for help with data collection and Jonathan Miller, Lynn Lohnas, and Ashwin Ramayya for helpful discussion and input.

References

Blumenfeld, R., Ranganath, C., 2007. Prefrontal cortex and long-term memory encoding: an integrative review of findings from neuropsychology and neuroimaging. Neuroscientist 13 (3), 280.
Burgess, A.P., Gruzelier, J.H., 1997. Short duration synchronization of human theta rhythm during recognition memory. Neuroreport 8, 1039–1042.
Burke, J.F., Zaghloul, K.A., Jacobs, J., Williams, R.B., Sperling, M.R., Sharan, A.D., et al., 2013. Synchronous and asynchronous theta and gamma activity during episodic memory formation. J. Neurosci. 33 (1), 292–304.
Burke, J.F., Long, N.M., Zaghloul, K.A., Sharan, A.D., Sperling, M.R., Kahana, M.J., 2013. Human intracranial high-frequency activity maps episodic memory formation in space and time. Neuroimage. http://dx.doi.org/10.1016/j.neuroimage.2013.06.067 (in press).
Crone, N., Boatman, D., Gordon, B., Hao, L., 2001. Induced electrocorticographic gamma activity during auditory perception. Clin. Neurophysiol. 112 (4), 565–582.
Crone, N.E., Miglioetti, D.L., Gordon, B., Sieracki, J.M., Wilson, M.T., Uematsu, S., et al., 1998a. Functional mapping of human sensorimotor cortex with electrocorticographic spectral analysis. I. Alpha and beta event-related desynchronization. Brain 121, 2271–2299.
Crone, N.E., Miglioretti, D.L., Gordon, B., Lesser, R.P., 1998b. Functional mapping of human sensorimotor cortex with electrocorticographic spectral analysis. II. Event-related synchronization in the gamma band. Brain 121 (12), 2301.
Crone, N.E., Korzeniewska, A., Franaszczuk, P., 2011. Cortical gamma responses: searching high and low. Int. J. Psychophysiol. 79 (1), 9–15.
Fell, J., Klaver, P., Lehnertz, K., Grunwald, T., Schaller, C., Elger, C.E., et al., 2001. Human memory formation is accompanied by rhinal–hippocampal coupling and decoupling. Nat. Neurosci. 4 (12), 1259–1264.
Fernandez, G., Effern, A., Grunwald, T., Pezer, N., Lehnertz, K., Dumpelmann, M., et al., 1999. Real-time tracking of memory formation in the human rhinal cortex and hippocampus. Science 285, 1582–1585.
Gevins, A., Smith, M.E., McEvoy, L., Yu, D., 1997. High-resolution EEG mapping of cortical activation related to working memory: effects of task difficulty, type of processing, and practice. Cereb. Cortex 7 (4), 374–385.
Gruber, T., Tsivilis, D., Montaldi, D., Müller, M., 2004. Induced gamma band responses: an early marker of memory encoding and retrieval. Neuroreport 15, 1837–1841.
Guderian, S., Schott, B., Richardson-Klavehn, A., Duzel, E., 2009. Medial temporal theta state before an event predicts episodic encoding success in humans. Proc. Natl. Acad. Sci. U. S. A. (13), 5365.
Hanslmayr, S., Staudigl, T., 2013. How brain oscillations form memories—a processing based perspective on oscillatory subsequent memory effects. NeuroImage. http://dx.doi.org/10.1016/j.neuroimage.2013.05.121 (in press).
Hanslmayr, S., Volberg, G., Wimber, M., Raabe, M., Greenlee, M.W., Bäumel, K.H.T., 2011. The relationship between brain oscillations and bold signal during memory formation: a combined EEG-fMRI study. J. Neurosci. 31 (44), 15674–15680.
Kahana, M.J., 2012. Foundations of Human Memory. Oxford University Press, New York, NY.
Kilner, J., Mattout, J., Henson, R., Friston, K., 2005. Hemodynamic correlates of EEG: a heuristic. Neuroimage 28 (1), 280–286.
Kim, H., 2011. Neural activity that predicts subsequent memory and forgetting: a meta-analysis of 74 fMRI studies. Neuroimage 54 (3), 2446–2461.
Klimesch, W., 1999. EEG alpha and theta oscillations reflect cognitive and memory performance: a review and analysis. Brain Res. Rev. 29, 169–195.
Klimesch, W., Doppelmayr, M., Schimke, H., Ripper, B., 1997. Theta synchronization and alpha desynchronization in a memory task. Psychophysiology 34 (2), 169–176.
Klimesch, W., Doppelmayr, M., Russegger, H., Pachinger, T., Schwaiger, J., 1998. Induced alpha band power changes in the human EEG and attention. Neurosci. Lett. 244 (2), 73–76.
Kovach, C.K., Tsuchiya, N., Kawasaki, H., Oya, H., Howard, M.A., Adolphs, R., 2011. Manifestation of ocular-muscle EMG contamination in human intracranial recordings. Neuroimage 54 (1), 213–233.
Lachaux, J.P., Axmacher, N., Mormann, F., Halgren, E., Crone, N.E., 2012. High-frequency neural activity and human cognition: past, present, and possible future of intracranial EEG research. Prog. Neurobiol. 98, 279–301.
Lega, B., Jacobs, J., Kahana, M., 2011. Human hippocampal theta oscillations and the formation of episodic memories. Hippocampus 22 (4), 748–761.
Lisman, J.E., Jensen, O., 2013. The theta-gamma neural code. Neuron 77 (6), 1002–1016.
Lohnas, L.J., Kahana, M.J., 2013. Parametric effects of word frequency effect in memory for mixed frequency lists. J. Exp. Psychol. Learn. Mem. Cogn. (in press).
Manning, J.R., Jacobs, J., Fried, I., Kahana, M.J., 2009. Broadband shifts in LFP power spectra are correlated with single-neuron spiking in humans. J. Neurosci. 29 (43), 13613–13620.
Matsumoto, J.Y., Stead, M., Kucewicz, M.T., Matsumoto, A.J., Peters, P.A., Brinkmann, B.H., et al., 2013. Network oscillations modulate interictal epileptiform spike rate during human memory. Brain 136, 2444–2456.
Miller, J.F., Kahana, M.J., Weidemann, C.T., 2012. Recall termination in free recall. Mem. Cogn. 40 (4), 540–550.
Miller, K.J., Leuthardt, E.C., Schalk, G., Rao, R.P.N., Anderson, N.R., Moran, D.W., Miller, J.W., Ojemann, J.G., 2007. Spectral changes in cortical surface potentials during motor movement. J. Neurosci. 27, 2424–2432.
Mitchell, D., McNaughton, N., Flanagan, D., Kirk, I., 2008. Frontal-midline theta from the perspective of hippocampal "theta". Prog. Neurobiol. 86 (3), 156.
Mizuhara, H., Wang, L.-Q., Kobayashi, K., Yamaguchi, Y., 2004. A long-range cortical network emerging with theta oscillation in a mental task. Neuroreport 15 (8), 1233–1238.
Morton, N.W., Kahana, M.J., Rosenberg, E.A., Sperling, M.R., Sharan, A.D., Polyn, S.M., 2013. Category-specific neural oscillations predict recall organization during memory search. Cereb. Cortex (in press).
Muthukumaraswamy, S.D., 2013. High-frequency brain activity and muscle artifacts in MEG/EEG: a review and recommendations. Front. Hum. Neurosci. 7.
Niessing, J., Ebisch, B., Schmidt, K.E., Niessing, M., Singer, W., Galuske, R.A.W., 2005. Hemodynamic signals correlate tightly with synchronized gamma oscillations. Science 309 (5736), 948–951.
Nunez, P.L., Srinivasan, R., 2006. Electric Fields of the Brain. Oxford University Press, New York.
Osipova, D., Takashima, A., Oostenveld, R., Fernndez, G., Maris, E., Jensen, O., 2006. Theta and gamma oscillations predict encoding and retrieval of declarative memory. J. Neurosci. 26 (28), 7523–7531.
Paller, K.A., Wagner, A.D., 2002. Observing the transformation of experience into memory. Trends Cogn. Sci. 6 (2), 93–102.
Paller, K.A., Kutas, M., Mayes, A.R., 1987. Neural correlates of encoding in an incidental learning paradigm. Electroencephalogr. Clin. Neurophysiol. 67, 360–371.
Pfurtscheller, G., Lopes Da Silva, F.H., 1999. Event-related EEG/MEG synchronization and desynchronization: basic principles. Clin. Neurophysiol. 110 (11), 1842–1857.
Sauseng, P., Hoppe, J., Klimesch, W., Gerloff, C., Hummel, F.C., 2007. Dissociation of sustained attention from central executive functions: local activity and interregional connectivity in the theta range. Eur. J. Neurosci. 25, 587–593.
Sederberg, P.B., Kahana, M.J., Howard, M.W., Donner, E.J., Madsen, J.R., 2003. Theta and gamma oscillations during encoding predict subsequent recall. J. Neurosci. 23 (34), 10809–10814.
Sederberg, P.B., Gauthier, L.V., Terushkin, V., Miller, J.F., Barnathan, J.A., Kahana, M.J., 2006. Oscillatory correlates of the primacy effect in episodic memory. Neuroimage 32 (3), 1422–1431.
Sederberg, P.B., Schulze-Bonhage, A., Madsen, J.R., Bromfield, E.B., McCarthy, D.C., Brandt, A., et al., 2007. Hippocampal and neocortical gamma oscillations predict memory formation in humans. Cereb. Cortex 17 (5), 1190–1196.
Serruya, M.D., Sederberg, P.B., Kahana, M.J., 2013. Power shifts track serial position and modulate encoding in human episodic memory. Cereb. Cortex (in press).
Shrager, Y., Kirwan, C., Squire, L., 2008. Activity in both hippocampus and perirhinal cortex predicts the memory strength of subsequently remembered information. Neuron 59 (4), 547.
Stoller, A., 1949. Slowing of the alpha-rhythm of the electro-encephalogram and its association with mental deterioration and epilepsy. Br. J. Psychiatry 95 (401), 972–984.
Voytek, B., Secundo, L., Bidet-Caulet, A., Scabini, D., Stiver, S.I., Gean, A.D., et al., 2010. Hemicraniectomy: a new model for human electrophysiology with high spatio-temporal resolution. J. Cogn. Neurosci. 22 (11), 2491–2502.
Wagner, A.D., Schacter, D.L., Rotte, M., Koutstaal, W., Maril, A., Dale, A.M., et al., 1998. Building memories: remembering and forgetting of verbal experiences as predicted by brain activity. Science 281, 1188–1191.
Weidemann, C.T., Mollison, M.V., Kahana, M.J., 2009. Electrophysiological correlates of high-level perception during spatial navigation. Psychon. Bull. Rev. 16 (2), 313–319.
Yuval-Greenberg, S., Tomer, O., Keren, A.S., Nelken, I., Deouell, L.Y., 2008. Transient induced gamma-band response in EEG as a manifestation of miniature saccades. Neuron 58 (3), 429–441.